Resolution of Three Structural States of Spin-Labeled Myosin in Contracting Muscle

E. Michael Ostap, Vincent A. Barnett, and David D. Thomas
Department of Biochemistry, University of Minnesota Medical School, Minneapolis, Minnesota 55455 USA

ABSTRACT We have used electron paramagnetic resonance (EPR) spectroscopy to detect ATP- and calcium-induced changes in the structure of spin-labeled myosin heads in glycerinated rabbit psoas muscle fibers in key physiological states. The probe was a nitroxide iodoacetamide derivative attached selectively to myosin SH1 (Cys 707), the conventional EPR spectra of which have been shown to resolve several conformational states of the myosin ATPase cycle, on the basis of nanosecond rotational motion within the protein. Spectra were acquired in rigor and during the steady-state phases of relaxation and isometric contraction. Spectral components corresponding to specific conformational states and biochemical intermediates were detected and assigned by reference to EPR spectra of trapped kinetic intermediates. In the absence of ATP, all of the myosin heads were rigidly attached to the thin filament, and only a single conformation was detected, in which there was no sub-microsecond probe motion. In relaxation, the EPR spectrum resolved two conformations of the myosin head that are distinct from rigor. These structural states were virtually identical to those observed previously for isolated myosin and were assigned to the populations of the M*·ATP and M**·ADP·P_i states. During isometric contraction, the EPR spectrum resolves the same two conformations observed in relaxation, plus a small fraction (20–30%) of heads in the oriented actin-bound conformation that is observed in rigor. This rigor-like component is a calcium-dependent, actin-bound state that may represent force-generating cross-bridges. As the spin label is located near the nucleotide-binding pocket in a region proposed to be pivotal for large-scale force-generating structural changes in myosin, we propose that the observed spectroscopic changes indicate directly the key steps in energy transduction in the molecular motor of contracting muscle.

INTRODUCTION

Force generation during muscle contraction arises from the direct interaction of myosin and actin, coupled to a cycle of ATP hydrolysis (Scheme 1). According to the rotating cross-bridge model, the molecular reorientation of the myosin head attached to actin produces strain, which is then relieved by the sliding motion of the myosin on actin filaments (Reedy et al., 1965; Huxley, 1969; Huxley and Simmons, 1971). The general hypothesis is that changes in the nucleotide at the myosin active site induce changes in the conformation of the myosin head, which change the interaction between myosin and actin in a way that results in directional sliding of the filaments (Taylor, 1979; Eisenberg and Hill, 1985; Hibberd and Trentham, 1986).

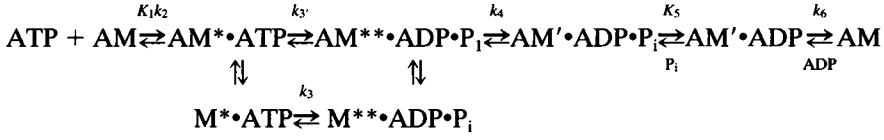

Scheme1

The central goal in muscle biophysics has been to detect the force-generating structural changes in the cross-bridge. Conformational changes within the myosin head during steady-state ATP hydrolysis have been detected by observing changes in UV absorbance (Morita, 1967), intrinsic fluorescence (Werber et al., 1972; Bagshaw et al., 1974; Trentham et al., 1976), biochemical cross-linking (Sutoh and Lu, 1987; Huston et al., 1988), electron paramagnetic resonance (EPR) spectroscopy (Seidel et al., 1970; Wells and Bagshaw, 1984; Barnett and Thomas, 1987), electron microscopy (Walker and Trinick, 1988; Katayama, 1989; Tokunaga et al., 1991), NMR spectroscopy (Shriver and Sykes, 1982), electrical birefringence (Highsmith and Eden, 1993), fluorescence energy transfer (Dalbey et al., 1983), and small-angle x-ray scattering (Wakabayashi et al, 1992).

Received for publication 5 July 1994 and in final form 20 April 1995.

Address reprint requests to Dr. David D. Thomas, Department of Biochemistry, University of Minnesota Medical School, Millard 4–225, 435 Delaware St., SE, Minneapolis, MN 55455. Tel.: 612-625-0957; Fax: 612-624-0632; E-mail: ddt@ddt.biochem.umn.edu.

Dr. Ostap's current address is Department of Cell Biology and Anatomy, The Johns Hopkins University School of Medicine, Baltimore, MD 21205.

Dr. Barnett's current address is Department of Physiology, University of Minnesota Medical School.

0006-3495/95/07/177/12 $2.00

The goal of these studies has been to correlate the conformational states of the myosin head with the specific biochemical intermediates in Scheme 1 and to ultimately correlate a conformational change with the force-generating transition.

The high-resolution crystal structure of the myosin head suggests that the power stroke arises from a series of domain movements within the myosin head (Rayment et al. 1993a,b). Therefore, to accurately assign conformational states to different biochemical states, a high resolution technique is required to resolve multiple conformational states that are defined by domain movements. This technique must be able to precisely quantitate the mole fractions of these states during the ATP hydrolysis cycle and site-specifically detect changes only in the myosin head so the conformational states can be detected in muscle fibers.

The motional resolution of the nitroxide EPR spectrum makes spin labels uniquely powerful in the study of the molecular dynamics of systems with multiple conformational states. Steady-state EPR spectroscopy has the ability to resolve more than one motionally distinct class of spin labels and to quantitate the relative concentrations of the motional classes (Ostap et al., 1993). Previous EPR studies of purified myosin heads labeled at Cys 707 (SH1) with an iodoacetamide spin label (IASL) have utilized this resolution by (1) showing the presence of nucleotide-dependent, motionally distinct states and (2) correlating the motional states with the M*·ATP and M**·ADP·P_i intermediates on the myosin ATPase pathway (Barnett et al., 1987; Ostap et al., 1993). SH1 is located in the heart of the motor domain of the myosin head, ideally situated to participate in communication among the actin- and ATP-binding sites and the light-chain-binding region. It has been proposed that conformational transitions in the vicinity of SH1 are responsible for large-scale structural changes within the head that result in ATP-dependent force generation (Rayment et al., 1993a,b). Therefore, information about the structural dynamics near SH1 in active muscle should be crucial for understanding the molecular mechanism of muscle contraction. Therefore, in the present study, we have specifically labeled myosin heads in skinned muscle fibers at SH1 to detect and resolve the conformational states of the myosin head during the different physiological states of the muscle fiber, including isometric contraction.

MATERIALS AND METHODS

Preparations and solutions

Psoas muscle from New Zealand white rabbits was dissected and glycerinated as described by Fajer et al. (1988). Myofibrils were prepared by homogenizing (eight times for 15 s each) glycerinated fibers with a Tekmar Tissumizer. Glycerinated psoas fibers were spin labeled specifically at Cys 707 (SH1) at 4°C as follows. Glycerinated fibers were dissected into 0.25- to 0.5-mm bundles in rigor buffer (RB; 130 mM potassium propionate, 20 mM MOPS, 1 mM EDTA, 2 mM $MgCl_2$, 1 mM NaN_3) and tied to glass rods. The fibers were washed sequentially, twice for 5 min in RB, 15 min in RB plus 0.5% Triton, and twice for 5 min in RB. The fibers were then incubated for 60 min in 60 μM 5,5′-dithio-bis(2-nitrobenzoic acid) (DTNB; Sigma Chemical Co., St. Louis, MO) in RB. The fibers were washed twice for 5 min in RB, then twice for 5 min in RB plus 10 mM tetrapotassium pyrophosphate (K_4PP_i). Fibers were then labeled for 60 min with 0.5 mM 4-(2-iodoacetamido)-2,2,6,6-tetramethyl-1-piperidinyloxy (IASL) in RB plus 10 mM K_4PP_i. After labeling, the fibers were washed three times for 5 min in RB plus 10 mM K_4PP_i and twice for 5 min in RB. DTNB was removed by incubating the fibers in RB plus 10 mM dithiothreitol for 15 min. The fibers were finally washed twice in RB for 5 min and then glycerinated for storage by washing three times for 10 min in a mixture of 50% glycerol and 50% RB.

The above spin-labeling procedure differs from our previous method (Thomas et al., 1980; Thomas and Cooke, 1980) in the omission of a post-labeling ferricyanide treatment and the addition of the reversible DTNB preblocking step. In fact, when spin labeling with IASL is carried out without either of these steps, the specificity of SH1 (Cys 707) labeling is >92% (Matta and Thomas, 1992; Matta, 1994), but a very small fraction of nonspecifically bound label contributes an isotropic EPR spectral component (corresponding to weakly immobilized labels) that hinders quantitative spectral analysis (data not shown). The treatment with ferricyanide after labeling was found to eliminate the signal from weakly immobilized spin labels (Thomas et al., 1980), but we have found that this treatment can alter fiber mechanical properties. Therefore, we switched to the DTNB preblocking method for the present study. The DTNB reaction is intended to block fast reacting SH groups distinct from SH1. As the binding of myosin to actin decreases the reactivity of SH1 (Duke et al., 1976), the DTNB reaction was carried out in rigor, and the spin-labeling reaction was carried out in the presence of pyrophosphate, as described above. High salt ATPase assays have shown that this DTNB reaction in rigor blocks some SH1 sites as well as non-SH1 sites (Roopnarine and Thomas, 1994), but the EPR spectra and high salt ATPase results reported below show that the stated goal is achieved; the final preparation contains only strongly immobilized spin labels bound to SH1.

Rigor solution contained 220 mM potassium propionate, 6.0 mM $MgCl_2$, 1.0 mM, EGTA, 20 mM MOPS (pH 7.0), or 20 mM EPPS (pH 8.0). The relaxing solution was 5.0 mM ATP, 50 mM creatine phosphate, 233 IU/ml creatine kinase, 60 mM potassium propionate, 6.0 mM $MgCl_2$, 1.0 mM EGTA, 20 mM MOPS (pH 7.0), or 20 mM EPPS (pH 8.0). The solution for isometric contraction was prepared by the addition of 1.5 mM $CaCl_2$ to the relaxing solution. A stock solution of 200 mM Na_3VO_4 (V_i) was prepared as described by Barnett and Thomas (1987).

ATP-γ-S [adenosine 5′-*O*-(3-thiotriphosphate)] was purchased from Boehringer Mannheim (Indianapolis, IN) and purified by high pressure liquid chromatography on a preparative Bio-Rad (Richmond, CA) MA7Q anion exchange column (2 cm × 10 cm). The ATP-γ-S was eluted with a linear gradient of 0–2.0 M triethylamine bicarbonate, pH 7.8 (Berger and Thomas, 1991). The eluted ATP-γ-S was then lyophilized, resuspended in distilled water, lyophilized again, and diluted to a final concentration of 50–100 mM. The ATP-γ-S concentration was determined spectrophotometrically at 259 nm, with an extinction coefficient of 15.1 mM^{-1} cm^{-1}.

Characterization of spin-labeled fibers

The extent and specificity of SH1 (Cys 707) labeling were determined by measuring high salt ATPase activities. ATPase activities were determined by measuring the production of inorganic phosphate (Lanzetta et al., 1979). The K/EDTA-ATPase activity of IASL-myofibrils was assayed at 25°C in a solution containing 5 mM EDTA, 0.60 M KCl, and 50 mM MOPS, pH 7.5. The Ca/K-ATPase activity was assayed at 25°C in a solution containing 10 mM $CaCl_2$, 0.60 M KCl, and 50 mM MOPS, pH 7.5.

EPR spectroscopy

EPR experiments were performed on a Bruker ESP 300 spectrometer (Bruker Instruments, Billerica, MA). EPR spectra of IASL-fibers were acquired with a TM_{110} cavity (ER4103 TM; Bruker Instruments) modified to accept a capillary tube oriented parallel or perpendicular to the static

magnetic field. Muscle fiber bundles (0.25 mm) were placed in 1-mm glass capillaries and held isometrically by surgical thread tied to the bundle ends. Solutions were continuously flowed over the fibers during the EPR experiments at a rate of 300 μl/min. EPR spectra were obtained by using a peak-to-peak modulation amplitude of 2.0 G and a microwave power of 20 mW. The temperature of the samples was maintained by using a variable temperature controller (ER4111; Bruker Instruments). All spectra were acquired at 22 ± 1.0°C, unless stated otherwise.

EPR data analysis

EPR spectra were acquired and digitized with the spectrometer's built-in microcomputer with ESP 1620 spectral acquisition software (Bruker Instruments). Digitized EPR spectra were analyzed on IBM-compatible computers with a program developed by Robert L. H. Bennett. All spectra were normalized to correspond to the same number of spins by dividing by the double integral of the EPR spectrum. Spectral subtractions were performed as described by Barnett and Thomas (1987). Effective rotational correlation times (τ_r) that assume isotropic rotational motion were determined by the comparison of spectral splittings, $2T'_{\parallel}$ (see Fig. 2) with calibration curves (McCalley et al., 1972; Thomas et al., 1975). Effective order parameters (S) were calculated assuming rapid restricted motion from $S = (T'_{\parallel} - T_o)/(T_{\parallel} - T_o)$, where T_o is the isotropic hyperfine splitting constant (Squire et al., 1989). When rapid restricted motion was assumed, the half-cone angle (θ_c) that describes the amplitude of the motion was calculated from the order parameter from $S = \frac{1}{2}(\cos\theta_c + \cos^2\theta_c)$.

Multicomponent EPR spectra (e.g., in relaxation and contraction) were analyzed to determine the identities and mole fractions of spectral components as follows. First, single-component basis (end-point) spectra ($V_i(H)$) were obtained by trapping the labeled myosin heads in conformational intermediates with ATP analogues. Then a composite spectrum consisting of a linear combination of spectra ($V(H) = \Sigma x_i V_i(H)$) was constructed and compared with the experimental spectrum (see Results). The mole fractions (x_i) were varied to minimize χ^2, as described previously (Fajer et al., 1988).

RESULTS

Specificity of spin labeling

The reaction of IASL with myosin in glycerinated fibers has been shown to be very specific for Cys 707 (SH1) under the described labeling conditions (Matta and Thomas, 1992; Matta, 1994). The modification of SH1 is known to cause changes in the myosin high salt ATPase activity (Sekine and Kielly, 1964), which can be measured directly in myofibrils (Crowder and Cooke, 1984). The inhibition of the K/EDTA-ATPase activity has been demonstrated to be a sensitive indicator of the fraction of SH1 and/or SH2 (Cys 697) groups modified, declining linearly with the increase in the percentage of heads with either or both of these SH groups modified (discussed by Roopnarine and Thomas, 1994). Also, specific modification of SH1 increases the Ca/K-ATPase activity by approximately a factor of 10, but modification of SH2 does not (Sekine and Kielly, 1964; Reisler et al, 1974; Crowder and Cooke, 1984). In the IASL-fibers used in this study, the K/EDTA-ATPase activity was inhibited by a factor of 0.70 ± 0.05 (f_{SH}), and Ca/K-ATPase activity was increased by a factor of 8.0 ± 2.2, indicating that most of the myosin heads have a spin label attached to SH1 (not SH2). This leaves open the possibility that some heads contain additional spin labels attached to sites that do not affect the ATPase activity. However, the number of spin labels bound per myosin head (determined as described by Roopnarine et al., 1993) was found to be 0.68 ± 0.08, precisely matching the fraction of heads with inhibited K/EDTA-ATPase, implying that virtually all of the spin labels are bound to SH1, to the exclusion of all other sites in the fiber (Matta and Thomas, 1992; Matta, 1994).

EPR spectra in rigor

Fig. 1 shows the EPR spectra recorded in rigor buffer (pH 8.0) of randomly oriented IASL-myofibrils (Fig. 1, top) and IASL-fibers oriented perpendicular (Fig. 1, center) and parallel (Fig. 1, bottom) to the magnetic field. Table 1 shows the parameters derived from these spectra. The value for $2T'_{\parallel}$ (Table 1, top) obtained from the myofibril spectrum (Fig. 1, top) is not significantly different from the rigid-limit value (Fajer et al., 1990b), and saturation-transfer EPR yields an effective rotational correlation time of several hundred microseconds for IASL-myofibrils in rigor (Thomas et al., 1980), so the spin label is quite rigidly immobilized with respect to the myosin head on the nanosecond time scale ($\tau_r > 1$ μs; Thomas et al., 1975). Therefore, the conventional EPR spectrum of IASL-fibers, in the absence of nucleotides, is sensitive only to the global orientation of the myosin head, not the rotation of the spin label relative to the myosin head.

The large differences between the spectra of fibers oriented perpendicular (Fig. 1, center) and parallel (Fig. 1, bottom) to the magnetic field indicates that the myosin-bound spin labels assume a preferred orientational distribution relative to the fiber axis in rigor. The intense and narrow low-field peak and the positive high-field peak observed in the parallel orientation indicate a single, narrow orientational distribution of spin labels with respect to the thin filament (Thomas and Cooke, 1980; Fajer et al.,

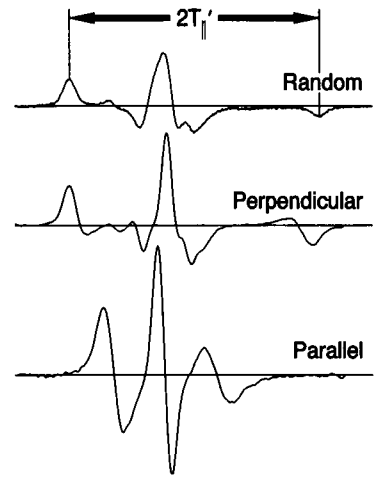

FIGURE 1 EPR spectra in rigor (pH 8.0) of randomly oriented IASL-myofibrils (top), and IASL-fibers oriented perpendicular (center) and parallel (third) to the magnetic field. The spectral splitting ($2T'_{\parallel}$) is defined in the top spectrum. All spectra have been normalized to correspond to the same number of spins.

TABLE 1 Spectral splittings and order parameters[a]

Sample[b]	$2T_{\parallel}'$	τ_r^{eff} [c]	S^{eff} [d]	θ_c^{eff} [e]
Myofibrils	70.20 ± 0.55 (4)	>1ms	1.0	0°
Parallel fibers	35.48 ± 0.41 (8)			
Perpendicular fibers, rigor	68.77 ± 0.17 (10)			
Perpendicular fibers, relaxation	66.39 ± 0.51 (8)			
Perpendicular fibers, contraction	68.21 ± 0.28 (9)			
Perpendicular fibers, ATP-γ-S	67.60 ± 1.10 (5)	60 ns	0.93	18°
Perpendicular fibers, ATP + V_i [f]	51.72 ± 0.88 (4)	9 ns	0.49	52°
S1 + ADP[g]	66.90 ± 0.42 (26)	50 ns	0.92	19°

[a] $T_{\parallel}'$ is defined in Fig. 1. Numbers in parentheses are the numbers of combined experiments for determination of the mean and standard deviation. τ_r^{eff}, S^{eff}, and θ_c^{eff} are not determined for samples in which more than one population of spins is evident.

[b] Results were independent of pH.

[c] Effective rotational correlation time, assuming isotropic ($S = 0$) rotational motion.

[d] Effective order parameter assuming rapid ($\tau_r \leq 0.1$ ns) restricted rotational motion.

[e] Half-cone angle for spin label wobble, calculated from S^{eff}.

[f] Spectral splittings determined from the spectrum with the immobile component subtracted (see Results).

[g] From Ostap et al. (1993).

1990b). The single orientational distribution reported by the EPR spectrum indicates that IASL is stereospecifically bound to a single site on the myosin head, thus supporting the kinetic evidence for the specific labeling of SH1.

EPR spectra in relaxation and contraction

The splitting of the EPR spectrum of perpendicular-oriented IASL-fibers decreased by 2.4 ± 0.7 G (Table 1) upon relaxation (Fig. 2, second spectrum), indicating that the spin labels are mobile relative to the myosin heads in the presence of ATP. This spectrum was unaffected by rotating the fibers to a parallel orientation (not shown), indicating that there is little or no orientational dependence of the spin labels on the EPR spectrum in relaxation, so differences between this spectrum and that of rigor myofibrils (Fig. 1, top) are caused entirely by nanosecond rotational motions within the head. This EPR spectrum is nearly identical with the spectrum of purified IASL-myosin heads (IASL-S1) in solution in the presence of ATP (Barnett and Thomas, 1987; Ostap et al., 1993), which has been shown to be a linear combination of two distinct populations of spin labels that are rotationally mobile on the nanosecond time scale (Barnett and Thomas, 1987; Ostap et al., 1993).

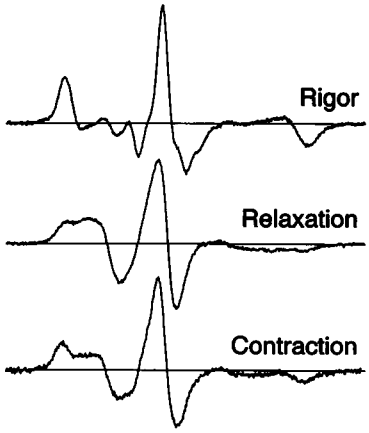

FIGURE 2 EPR spectra of IASL-fibers oriented perpendicular to the magnetic field in rigor, relaxation, and contraction at pH 8.0. The rigor spectrum is defined as component 1.

When 1.5 mM Ca^{2+} was added to the relaxing solution, causing isometric contraction, the splitting of the EPR spectrum (Fig. 2, third spectrum) increased by 1.8 ± 0.8 G (Table 1), indicating that at least a fraction of the spin labels became more rigidly bound to the myosin head. In contrast to relaxation, the EPR spectrum of contracting IASL-fibers oriented parallel to the magnetic field (data not shown) is not the same as in the perpendicular orientation, indicating that the spectrum is also complicated by the orientation (roughly rigor-like) of a small population of spin labels. Saturation experiments in which ATP concentrations were increased to 20 mM or creatine phosphate concentrations were increased to 70 mM did not significantly change the EPR spectrum, indicating that the substrate concentrations are at saturating levels. Therefore, the spectral changes observed in isometric contraction are not a result of a rigor core in the fiber bundles, but are a result of changes of the conformational states of the nucleotide-bound myosin heads that are presumably intermediates in the actomyosin ATPase cycle. The spectrum in contraction appears to be intermediate between the spectra in rigor and relaxation. Additional analysis is required to determine whether this spectrum in contraction reports more than one population of spin labels that are rotationally dynamic on the nanosecond time scale (below).

EPR spectra of trapped intermediates

To resolve and quantitate the spectral components corresponding to intermediate conformational states, we first obtained EPR spectra under conditions designed to trap intermediates of the ATPase cycle (Scheme 1). It has been proposed that ATP-γ-S traps the myosin head in a complex that is a conformational analogue of the M·ATP state (Goody and Hofmann, 1980). The spectral splitting ($2T_{\parallel}' = 67.6 \pm 1.1$ G; Table 1) of IASL-fibers in the presence of 10 mM ATP-γ-S (Fig. 3, second spectrum) is similar to that observed in relaxation. This splitting corresponds to an effective rotational correlation time of $\tau_r^{eff} = 60$ ns, assuming isotropic rotational motion (McCalley et al., 1972). Alternatively, assuming rapid ($\tau_r \geq 0.1$ ns) restricted motion, the half-cone angle (θ_c) that describes the amplitude of the spin label's rotational motion increases from the rigor value of $\theta_c = 0°$ to $\theta_c^{eff} = 18°$ (Table 1). Thus, the actual τ_r is ≥50 ns, and the actual θ_c is ≥20°. To ensure nucleotide saturation, the EPR spectra of IASL-fibers in the presence of ATP-γ-S were acquired at 4°C (Kraft et al., 1992). Increasing the ATP-γ-S concentration or further reduction

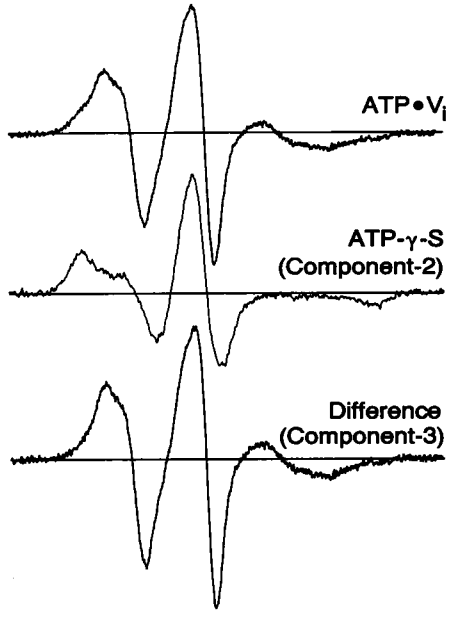

FIGURE 3 EPR spectrum of perpendicular-oriented fibers in relaxing solution plus 5 mM V_i, pH 8.0 (*top*) and in rigor solution plus 10 mM MgATP-γ-S at 4°C, pH 8.0 (*center*). The latter spectrum is defined as component 2. The third spectrum (*bottom*) shows the difference spectrum obtained by subtracting 27% of the center spectrum from the top spectrum. This difference spectrum is defined as component 3. All spectra have been normalized to correspond to the same number of spins.

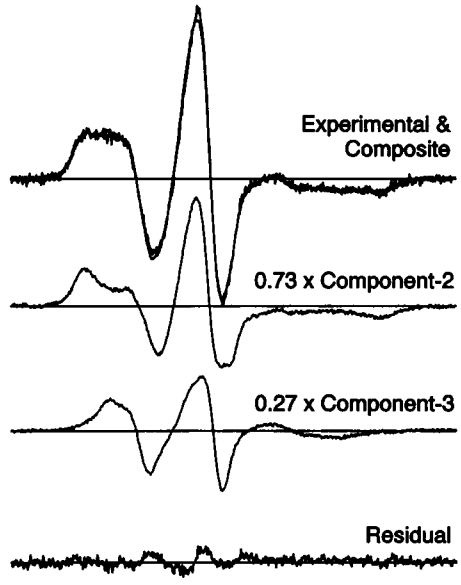

FIGURE 4 Multicomponent EPR spectral analysis of IASL-fibers in relaxation (pH 7.0), oriented perpendicular to the magnetic field. At the top is an overlay of the spectrum in relaxation and a composite spectrum that is the best fit to Eq. 1 ($x_1 = 0$, $x_2 = 0.73 \pm 0.03$, and $x_3 = 0.27 \pm 0.03$); i.e., the composite spectrum is a linear combination of 73% of component 2 (second spectrum, $V_2(H)$ in Eq. 1) and 27% of component 3 (third spectrum, $V_3(H)$ in Eq. 1), as summarized in Table 2. The bottom spectrum is a residual spectrum obtained by the subtraction of the composite spectrum from the relaxation spectrum. All spectra have been normalized to correspond to their respective mole fractions.

of the temperature did not significantly change the splitting or the line shape of the EPR spectrum. This EPR spectrum is virtually identical to spectrum of purified IASL-myosin heads (IASL-S1) in the presence of either ATP-γ-S or ADP (Barnett and Thomas, 1987; Ostap et al., 1993). We conclude that the conformation of myosin, as detected by IASL at SH1, that predominates in the M·ATP state is indistinguishable from that of the M·ADP state (Barnett and Thomas, 1987). Therefore, for further analysis of multicomponent spectra, we will use the spectrum of IASL-S1 plus 5 mM ADP (Fig. 4, second spectrum; Table 1) to represent this conformational state. The spectrum of IASL-S1 plus ADP has a better signal-to-noise ratio than that of IASL-fibers plus ATP-γ-S, allowing for more precise spectral analysis.

The addition of 5 mM orthovanadate (V_i) to the relaxing solution traps the myosin head in a complex that has been proposed to be a conformational analogue of the M·ADP·P_i state, a key intermediate in the ATP hydrolysis reaction (Goodno, 1979; Dantzig and Goldman, 1985). The spectral splitting ($2T'_{\parallel} = 51.72 \pm 0.88$; Table 1) of the EPR spectrum of IASL-fibers plus ATP and V_i (Fig. 3, top spectrum) is less than that of IASL-fibers in rigor, relaxation, or contraction, indicating further mobilization of the spin labels relative to the myosin head. The addition of 5 mM V_i and 5 mM ADP to rigor IASL-fibers does not change the EPR spectrum significantly, supporting the finding that ADP and vanadate added to rigor fibers do not cause relaxation (Dantzig and Goldman, 1985).

Resolution of spectral components and conformational states

It has been demonstrated previously that the EPR spectrum of purified IASL-myosin heads in the presence of ATP reports multiple spectral components that represent distinct populations of spin labels that are rotationally mobile on the nanosecond time scale. These motionally distinct spin label populations represent conformational states of the myosin heads that can be correlated directly with specific biochemical intermediates (Barnett and Thomas, 1987; Ostap et al., 1993).

Digital spectral analysis was used to resolve and quantitate the spectral components that represent different spin label mobilities and, probably, different conformational states of the myosin head. To best resolve the spectral components present during relaxation and contraction, IASL-fibers oriented perpendicular to the magnetic field were used rather than IASL-fibers oriented parallel to the magnetic field. For the remainder of this paper, the rigidly bound, highly oriented population of spin labels observed in rigor will be referred to as component 1 (Fig. 2, top). The slightly mobile population of probes that are randomly oriented with the intermediate spectral splitting, observed for fibers in the presence of ATP-γ-S or for IASL-S1 in the presence of ADP or ATP-γ-S, will be referred to as component 2 (Fig. 3, middle). The highly mobile component that is randomly oriented with the smallest spectral splitting,

predominant in the presence of ATP plus V_i, will be referred to as component 3.

With IASL-S1 plus ADP as a model for component 2, computer subtraction was used to quantitate the relative concentrations of the two motional components in the ATP plus V_i spectrum and to obtain the spectrum of component 3 (Barnett and Thomas, 1987; Ostap et al., 1993). Component 2 was subtracted from the ATP plus V_i spectrum (Fig. 3, top) until the intensity from the spectral wings was removed without distorting the central line (Ostap et al., 1993). This procedure results in a well defined, unambiguous end point (Fig. 3, bottom), as shown previously for IASL-myosin (Barnett and Thomas, 1987) and IASL-S1 (Ostap et al., 1993) in the presence of nucleotides. This end point will be used as a model for the population of highly mobile spin labels (component 3) in subsequent analyses. The splitting of this component ($2T'_{\parallel}$ = 51.7 ± 0.9 G) corresponds to $\tau_r \leq 9$ ns and $\theta_c \geq 52°$ (Table 1). The result of this subtraction (Table 2) shows that the spectrum of IASL-fibers in the presence of saturating ATP plus V_i is composed of 27 ± 5% of component 2 and 73 ± 5% of component 3.

The EPR spectra of IASL-fibers in relaxation and contraction were modeled as a linear combination of components 1, 2, and 3 by using the following equation:

$$V(H) = \sum_{i=1}^{3} x_i V_i(H) \qquad (1)$$

where $V(H)$ is the composite EPR spectrum, i.e., V is the spectral intensity at magnetic field position, H; $V_1(H)$, $V_2(H)$, $V_3(H)$ are the EPR spectra of components 1, 2, and 3; and x_1, x_2, and x_3 are the mole fractions of the components in $V(H)$. The mole fractions were varied to minimize χ^2 between this composite spectrum and the experimental spectrum.

The fit of the spectrum in relaxation (Fig. 4, top) to Eq. 1 was excellent (see composite and difference spectra in Fig. 4), with $x_1 = 0$ (i.e., no contribution from the rigor-like component 1), $x_2 = 0.73 \pm .03$, and $x_3 = 0.27 \pm .03$. Thus the spectrum in relaxation contains the same two motional components (2 and 3) as in the presence of ATP and V_i (Fig. 3, top spectrum), but the fractions of the components are very different (Table 2). At pH 8.0, the spectrum is also fit very well by a linear combination of component 2 (x_2 = 0.60 ± 0.06) and component 3 (x_3 = 0.40 ± 0.06; Table 2). There is no contribution of component 1 in the spectrum of relaxed IASL-fibers at pH 7.0 or pH 8.0.

Dividing the mole fraction of component 3 (x_3) by the mole fraction of component 2 (x_2) results in an apparent equilibrium constant (K_3^{app} = 0.37 ± 0.04 at pH 7.0, 0.67 ± 0.18 at pH 8.0; Table 2) that is approximately the same as determined from EPR spectra of purified IASL-S1 plus ATP in solution (K_3^{app} = 0.45 ± 0.06 at pH 7.0, 0.75 ± 0.03 at pH 8.0; Ostap et al., 1993), which agrees with the equilibrium constant (K_3; Scheme 1) for the hydrolysis of ATP by myosin (Barnett and Thomas, 1987; Ostap et al., 1993). Therefore, it appears that, during ATP hydrolysis, *in the muscle fiber as well as in isolated myosin, component 2 and component 3 represent the conformations of myosin heads that predominate in the (A)M**ATP and (A)M***ADP·P_i* state, respectively (Barnett and Thomas, 1987; Ostap et al., 1993).

The fit of the spectrum in isometric contraction at pH 7.0 (Fig. 5, top) to Eq. 1 is excellent (see composite and difference spectra in Fig. 4), with $x_1 = 0.27 \pm .06$, $x_2 = 0.53 \pm .06$, and $x_3 = 0.20 \pm .06$. Thus the spectrum in contraction contains the same two components (2 and 3) with nanosecond mobility that are observed in relaxation plus a substantial contribution from the immobile rigor-like component (component 1). At pH 8.0, the contraction spectrum is also a linear combination of component 1 (x_1 = 0.28 ± 0.04), component 2 (x_2 = 0.43 ± 0.04), and component 3 (x_3 = 0.29 ± 0.04; Table 2). The apparent equilibrium constant for ATP hydrolysis, $K_3^{app} = x_3/x_2$, agrees with that measured in relaxation, at both pH 7.0 and pH 8.0 (Table 2), indicating that component 2 and component 3 have the same relative populations in contraction and relaxation.

We also fit the spectrum of contracting IASL-fibers (Fig. 6, top) to a linear combination of component-1 (i.e., rigor; Fig. 6, second spectrum) and the spectrum of relaxed fibers (Fig. 6, third spectrum). The fits were excellent at both pH 7.0 and 8.0, with the mole fractions $x_1 = 0.27 \pm 0.06$ at pH 7.0 and x_1 = 0.28 ± 0.04 at pH 8.0. This result is in excellent agreement with the three-component analysis (Fig. 5), and confirms the conclusion that components 2 and 3 have the same relative concentrations (i.e., the same K_3^{app}) in relaxation and contraction.

TABLE 2 Relative populations of the three motional components detected during relaxation and contraction in IASL-fibers

Sample[a]	x_1	x_2	x_3	K_3^{app}[b]
IASL-fiber, pH 7.0				
Relaxation (11)	0	0.73 ± 0.03	0.27 ± 0.03	0.37 ± 0.04
Contraction (9)	0.27 ± 0.06	0.53 ± 0.06	0.20 ± 0.06	0.38 ± 0.12
IASL-fiber, pH 8.0				
ATP + V_i (4)	0	0.27 ± 0.05	0.73 ± 0.05	2.7 ± 0.12
Relaxation (9)	0	0.60 ± 0.06	0.40 ± 0.06	0.67 ± 0.18
Contraction (4)	0.28 ± 0.04	0.43 ± 0.04	0.29 ± 0.04	0.67 ± 0.11

[a] Numbers in parentheses are the numbers of combined experiments for the determination of the mean and standard deviation.
[b] K_3^{app} is x_3/x_2.

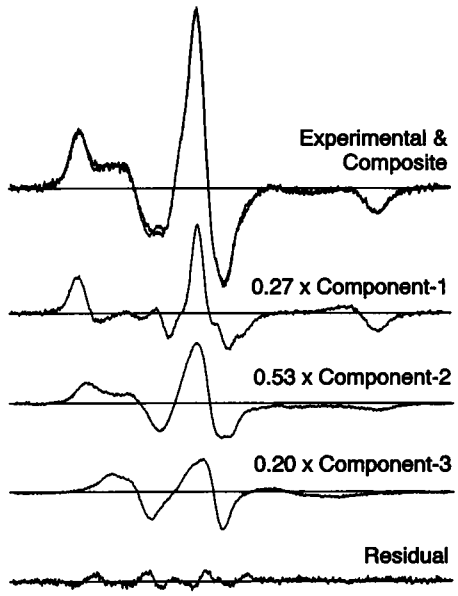

FIGURE 5 Multicomponent EPR spectral analysis of IASL-fibers in isometric contraction (pH 7.0), oriented perpendicular to the magnetic field. At the top is an overlay of the spectrum in contraction and a composite spectrum that is the best fit to Eq. 1 ($x_1 = 0.27 \pm 0.06$, $x_2 = 0.53 \pm 0.06$, and $x_3 = 0.20 \pm 0.06$); i.e., the composite spectrum is a linear combination of 27% of component 1 (second spectrum, $V_1(H)$), 53% of component 2 (third spectrum, $V_2(H)$), and 27% of component 3 (third spectrum, $V_3(H)$), as summarized in Table 2. The bottom spectrum is a residual spectrum obtained by the subtraction of the composite spectrum from the contraction spectrum. All spectra have been normalized to correspond to their respective mole fractions.

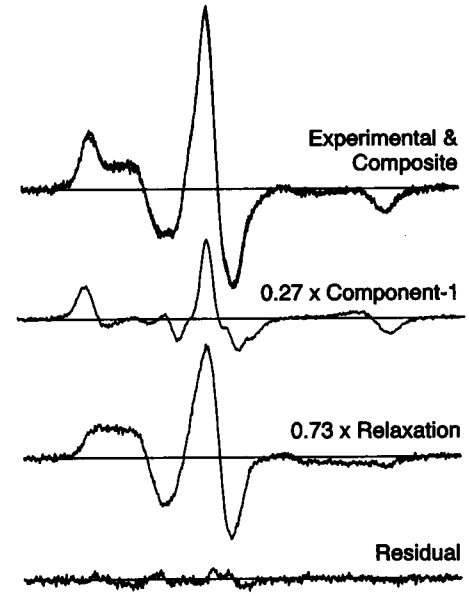

FIGURE 6 Analysis of the contraction spectrum as a linear combination of rigor and relaxation. At the top is an overlay of a spectrum of contracting IASL-fibers (pH 7.0), oriented perpendicular to the magnetic field, and a composite spectrum that is the best fit to a linear combination of 27% of the spectrum in rigor (second spectrum, component 1) and 73% of the spectrum in relaxation (third spectrum). At the bottom is a residual spectrum obtained by the subtraction of the composite spectrum from the contraction spectrum. All spectra have been normalized to correspond to their respective mole fractions.

DISCUSSION

The motional resolution of the nitroxide EPR spectrum makes spin labels uniquely powerful in the study of the molecular dynamics of systems with more than one motional class. Steady-state EPR spectroscopy has the ability to (1) resolve more than one motionally distinct class of spin labels and (2) quantitate the relative concentrations of the motional classes (Ostap et al., 1993). Previous EPR studies of purified myosin heads labeled at SH1 with IASL have utilized this resolution by (1) showing the presence of nucleotide-dependent motionally distinct states and (2) quantitating their relative concentrations, thus allowing for the correlation of these conformational states with the predominant intermediates on the myosin ATPase pathway (Barnett and Thomas, 1987; Ostap et al., 1993). In the present study, we have used EPR to detect and quantitate these conformational states directly in the different physiological states of the muscle fiber.

The rigorous analysis of the EPR spectra is facilitated by the site-specific labeling of SH1 by IASL. This is shown not only by the high salt ATPase inhibition and spin quantitation, as discussed in Results, but also by the EPR spectrum of rigor IASL-fibers oriented parallel to the magnetic field (Fig. 1, third spectrum), which shows a single, narrow orientational distribution of spin labels with respect to the fiber axis (Thomas and Cooke, 1980; Fajer et al., 1990b). This spectrum is identical with the spectrum of unlabeled fibers with IASL-S1 bound to the thin filament (data not shown), indicating that IASL is bound only to the myosin heads. *Therefore, the spectral changes observed in this study are a result only of conformational changes detected at or near SH1 on the myosin head.*

The two spectral components that represent spin labels rotating on the nanosecond time scale (components 2 and 3; Table 1) are independent of the fiber orientation and report only the motion of the spin labels relative to the myosin head, not global head orientation or motion (Barnett and Thomas, 1987; Ostap et al., 1993). The increased nanosecond rotational motion of the spin labels is a result of internal conformational changes in the myosin head that either mobilize Cys 707 on the nanosecond time scale or change the protein environment surrounding the spin label, thus allowing the probe to undergo large-amplitude nanosecond rotational motion (Table 1; Ostap et al., 1993). Unlike components 2 and 3, component 1 represents spin labels that are rigidly bound to the myosin heads and highly oriented as in rigor. Although this rigor-like component complicates the EPR spectrum by adding orientational dependence, the orientational effects actually improve the resolution of component 1 from the other two spectral components when the fiber is oriented perpendicular to the magnetic field (Fig. 5). If the experiments were performed with IASL-fibers oriented parallel to the magnetic field, the contraction spectrum would appear as a linear combination of components 2 and 3, plus the parallel rigor spectrum (Fig. 1, bottom).

Interpretation of spectra in relaxation

The relaxation spectrum can be fit to a linear combination of two motionally distinct conformational states (Fig. 4, Table 2). This spectrum is nearly identical with the spectrum of IASL-S1 in solution in the presence of ATP (Barnett and Thomas, 1987; Ostap et al., 1993). Conformational states other than component 2 or component 3 are not detectable in the steady-state relaxation spectrum. Of course, there is not necessarily a one-to-one correspondence between the spectroscopically detected protein conformational states and the biochemical intermediates depicted in Scheme 1; i.e., each biochemical intermediate can correspond to a mixture of conformational states. Nevertheless, steady-state and transient EPR studies of purified IASL-myosin heads in in the presence of ATP have shown that component 2 and component 3, corresponding to myosin conformational states, are predominant in the M·ATP and the M·ADP·P_i biochemical intermediates of the myosin head, respectively (Barnett and Thomas, 1987; Ostap et al., 1993). Those studies also showed that the ratio of component 3 to component 2 (K_3^{app}; Table 2) is in good agreement with the equilibrium constant for the ATP hydrolysis step of myosin (K_3; Scheme 1). The K_3^{app} determined for relaxed fibers is approximately the same as K_3^{app} determined for purified IASL-S1 in solution. We conclude that the equilibrium constant for ATP hydrolysis is essentially the same in relaxed IASL-fibers as in IASL-S1, in agreement with previous biochemical measurements on unlabeled fibers (Ferenczi, 1986).

Because of perturbations caused by the modification of SH1, the values for K_3 determined for IASL-S1 (Ostap et al., 1993) and IASL-fibers (this study) are 10–15 times less than the values determined for unlabeled myosin heads in solution (Bagshaw et al., 1974) and fibers (Ferenczi et al., 1984). The attachment of IASL to SH1 in S1 results in three major perturbations of the ATPase cycle (Scheme 1): 1) a decrease in the rate ($k_{+3} + k_{-3}$) of ATP hydrolysis, 2) a decrease in the equilibrium constant (K_3) of the ATP hydrolysis step, and 3) a change in the rate of product release (k_4; Sleep et al., 1981; Ostap et al., 1993). The major result of these perturbations is the shift of the predominant steady-state intermediate from the M·ADP·P_i state to the M·ATP state (Ostap et al., 1993). Although the biochemical kinetics are significantly changed by modification of SH1, fully labeled IASL-fibers generate force. In fully labeled IASL-fibers, in isometric contraction, the ATPase rate is decreased by 48 ± 8%, and the tension is decreased by 68 ± 4% compared with unmodified fibers (Matta and Thomas, 1992; Matta, 1994; Bell et al., 1993).

Interpretation of spectra in contraction

The effect of activation by calcium is simply the addition of a small rigor-like component to the spectrum, so that three distinct spectral components (conformational states) are resolved. As the apparent equilibrium constant for ATP hydrolysis, K_3^{app} ([component 3/component 2]), is essentially the same for relaxation and contraction (Table 2), it is likely that it is equal to the actual equilibrium constant and that this constant is unaffected by interaction with actin ($K_3^{app} = K_3 = K_3'$, see Scheme 1). Analysis of Scheme 1 shows that, for this to be true, K_4 must not be much greater than 1 (if k_5 is rate limiting), or k_4 must be significantly less (~10 times) than the ATP hydrolysis rate (k_3). Therefore, it is likely that $K_4 < 1$, as shown previously for unlabeled fibers (Dantzig et al., 1992), and that there is at least one step after hydrolysis that is comparable with or slower than k_3 (Ferenczi et al., 1984).

We propose the model in Fig. 7 to explain how conformational transitions among these three components might be coupled to force generation. Myosin conformational states are assumed to correspond to the EPR components reported by IASL, indicated by shading of the heads in Fig. 7. Component-1 is predominant in the AM and AM′·D states, component 2 in the (A)M*·T state, and component 3 in the (A)M**·D·P_i state. Thus components 2 and 3 are weakly binding states that do not bear force but do undergo a two-step conformational change in which the IASL probe becomes more mobile as a result of a structural change in the vicinity of SH1 that results in increased bending of the head. The curved arrows indicate global orientational disorder on the microsecond time scale in states 2 and 3, but the mean (preferred) orientation of the actin-binding portion of the head remains essentially constant. Force generation is a transition from the weakly binding state 3 (AM**·D·P_i) to the strongly binding state 1 (AM′·D), in which the SH1 region becomes more rigid, the head becomes less bent, and the attachment of the head to act in becomes rigid and stereospecific. This model is consistent with the EPR data from IASL-fibers in rigor, relaxation, and contraction, as reported in the present study, and with other spectroscopic, physiological, and structural results (Thomas et al., 1995).

Relationship to other studies

The proposed overall (global) disorder and microsecond rotational dynamics of myosin heads in components 2 and 3, depicted by the curved arrows in Fig. 7, is based primarily on EPR and optical studies with other probes. Components 2 and 3 are characterized by nanosecond rotation of the spin label relative to the myosin head and therefore provide little direct information about the myosin head's global orientation or rotational dynamics. However, complementary experiments with SH1-bound maleimide spin labels (MSL), indane-dione spin labels (InVSL), or phosphorescent dyes, which bind rigidly to myosin heads even in the presence of ATP and report the global behavior of myosin heads, can be compared directly with this study. In agreement with the present study on IASL-fibers, the EPR spectrum of SH1-bound MSL (Thomas and Cooke, 1980; Fajer et al., 1990a,b) or InVSL (Roopnarine et al., 1993; Roopnarine and Thomas, 1994) reports a single, rigid, orientational

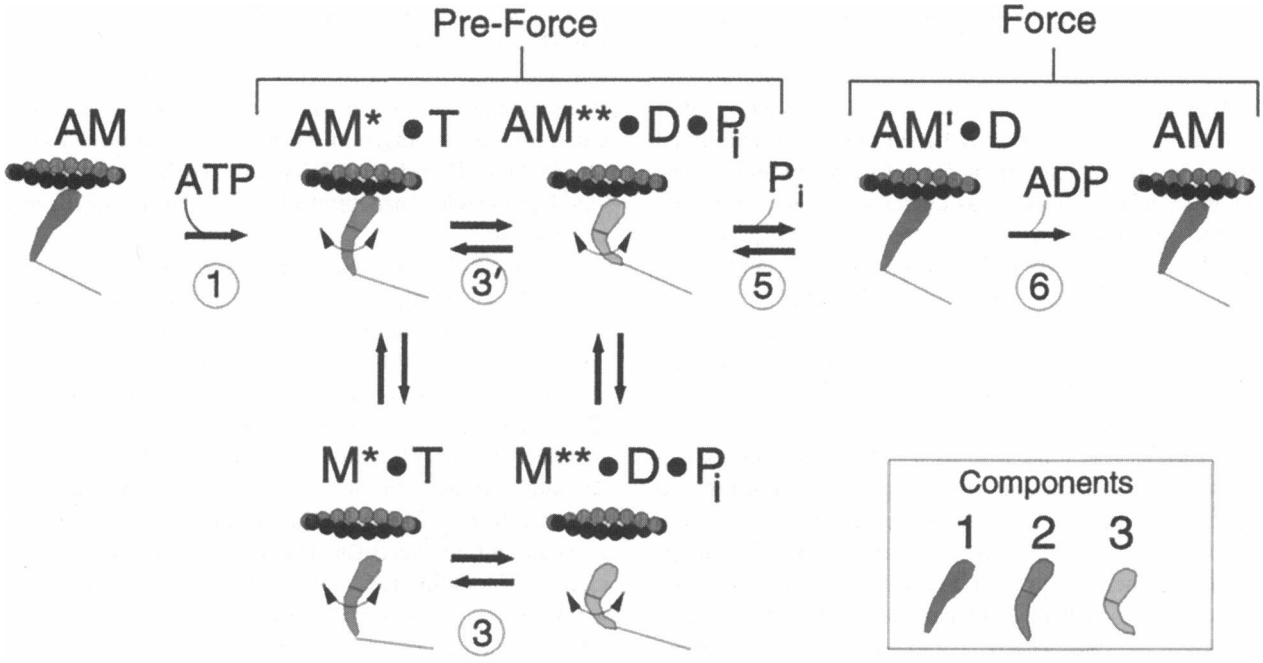

FIGURE 7 A model for the coupling of myosin conformational transitions to the ATPase cycle in contracting muscle. Intermediates and step numbers are defined as in Scheme 1, except that ATP and ADP are abbreviated as T and D, respectively. Myosin conformational states, corresponding to IASL EPR spectral components with different internal nanosecond mobilities, are coded by shading and internal bending of the heads as indicated in the inset. The curved arrows indicate global orientational head disorder on the microsecond time scale in states 2 and 3. Force generation is a transition from AM**·D·P_i to AM'D, in which the SH1 region becomes more rigid, the head becomes less bent, and the attachment of the head to actin becomes rigid and stereospecific.

distribution in rigor. In relaxation, both spin labels show substantial orientational disorder, and saturation transfer EPR (Thomas et al., 1980; Barnett and Thomas, 1989; Roopnarine and Thomas, 1995) and phosphorescence (Stein et al., 1990; Thomas et al., 1995) measurements indicate that these myosin heads are rotationally mobile on the microsecond time scale. Therefore, we conclude that the myosin heads that are represented by components 2 and 3 are also dynamically disordered on the microsecond time scale, as depicted in Fig. 7.

In isometrically contracting fibers labeled with MSL or InVSL, a linear combination of disordered and rigor-like myosin heads is observed (Cooke et al., 1982; Fajer et al., 1990c; Roopnarine and Thomas, 1995). Saturation transfer EPR (Barnett and Thomas, 1989; Roopnarine and Thomas, 1995) and phosphorescence (Stein et al., 1990; Thomas et al., 1995) experiments indicate that the disordered heads are mobile on the microsecond time scale and that the oriented heads are rigidly attached to the actin filament. In all of these studies of global head dynamics, the fraction of heads in the rigor-like state during contraction (10–20%) is similar to the fraction of component 1 observed in the present study (Table 2). As IASL, MSL, and InVSL are attached to the same site on the myosin head (SH1), the rigor-like component being detected in isometric contraction by MSL and InVSL is probably the same population of myosin heads that is represented by component 1. This would indicate that components 2 and 3 represent the myosin heads that are dynamically disordered in contraction as well as in relaxation. The results of the present study indicate that components 2 and 3 represent the non-force-producing states ((A)M*·ATP and (A)M**·ADP·P_i), so the dynamically disordered component in the MSL and InVSL experiments must also represent the non-force-producing states. A crucial question is whether a substantial fraction of these dynamically disordered (both globally and internally) heads are attached to actin, as depicted in Fig. 7. This question remains to be answered for IASL, but the answer is yes for MSL, based on EPR experiments on relaxed muscle fibers at low ionic strength (Fajer et al., 1991) and in the presence of (Berger et al., 1989) or ATP-γ-S in solution (Berger and Thomas, 1991) and myofibrils (Berger and Thomas, 1993, 1994). Therefore, if component 1 represents only the force-generating state, then the EPR data suggests that *the cross-bridge power stroke is a transition from a dynamically disordered (both internally and globally) state of the myosin head to a highly oriented, rigor-like state* (Fig. 7) as proposed previously (Berger and Thomas, 1994; Thomas et al., 1995). As pointed out by Berger and Thomas (1994), this disorder-to-order transition would be enough to produce force, without the need to invoke a large-scale shape change in the head like the one depicted in Fig. 7.

It is important to ask whether the dynamic disorder of actin-attached heads, as suggested by EPR of probes at SH1, is confirmed by methods that report the behavior of the whole myosin head. Rapid-freeze electron microscopy studies of purified actomyosin solutions (Pollard et al., 1993) suggest that actin-attached myosin heads in the preforce-

generating states are in the rigor-like orientation. This result seems to contradict the disorder-to-order hypothesis. However, other electron microscopy studies in solution (reviewed by Thomas, 1994; Walker et al., 1994, 1995) and in fibers (Hirose et al., 1993) provide support for orientational disorder of attached heads in preforce (weak-binding) states, even before ATP hydrolysis, as depicted in Fig. 7. Furthermore, the dynamic disorder detected by SH1 probes in contraction is similar to that observed by optical probes on the regulatory light chain (Thomas et al., 1995).

If the disorder-to-order transition depicted in Fig. 7 does not occur, or is not sufficient for force generation, then the myosin head shape change depicted becomes a more essential part of the model of force generation. In fact, the original EPR observation with MSL-fibers, that no distinct head angle other than the rigor angle was observed in contraction (Cooke et al., 1982), gave support years ago to the proposal that the head has two domains, one that keeps a constant orientation on actin and another that rotates and thus results in a bent head that makes force (Huxley and Kress, 1985; Cooke, 1986). Although there is no direct information from the present IASL EPR data for a large-scale change in myosin head shape, it is quite plausible that the changes in probe mobility coincide with the nucleotide-induced changes in myosin head shape (interpreted as bending) deduced from fluorescence anisotropy (Aguirre et al., 1989), electric birefringence (Highsmith and Eden, 1990, 1993), and x-ray scattering (Wakabayashi et al., 1992) studies on isolated myosin heads (S1) in solution. The key advance of the present study is a means of detecting these structural changes with site-directed probes as they occur in contracting muscle.

It has been shown that actin-attached, pre-force-generating myosin heads are important in the mechanism of contraction (Kress et al., 1986; Dantzig et al., 1988; Brenner et al., 1991; Poole et al., 1991; Kraft et al., 1992). Knowing the structure and conformational states of these heads is essential for understanding the mechanism of contraction. Therefore, it is important to test further the hypotheses suggested by Fig. 7. Steady-state EPR experiments wih ATP analogues (Fajer et al., 1988; Berger and Thomas, 1994) and transient EPR experiments (Ostap et al., 1993) correlated with transient mechanical studies (Bell et al., 1993) are required to make more precise interpretations of the spectral components.

Relationship to the high resolution crystal structure of S1

The high resolution crystal structure of the myosin head (Rayment et al., 1993a) locates both SH1 (Cys 707) and SH2 (Cys 697) on opposite sides of an α-helix in the 20-kDa fragment. This region is located in the heart of the motor domain of the myosin head, ideally situated to participate in communication among the actin- and ATP-binding sites and the light-chain-binding region. Biochemical cross-linking studies demonstrate that the region containing SH1 and SH2 can move >10 Å upon ATP binding in the absence of actin (Huston et al., 1988). The only way for these residues to be cross-linked would be for significant structural changes in the α-helix to occur (Rayment et al., 1993a). Therefore, SH1-bound IASL is optimally located to detected structural changes that are necessary for contraction.

With the information available in the S1 crystal structure, a model describing the structural basis of force generation has been proposed (Rayment et al., 1993b) and refined based on the structures of S1 fragments containing trapped nucleotide analogues (Fisher et al., 1995). This model predicts significant structural changes in the vicinity of SH1 that accompany ATP binding (step 1), ATP hydrolysis (step 3), and product release (steps 5 and 6). It suggests, as depicted in Fig. 7, that the initial attachment of S1 to actin is weak and not stereospecific and that two conformational changes, including reversible changes in S1 shape, result in a strong and stereospecific bond that completes the generation of force. The EPR results of the present study complement the x-ray data. EPR has sufficient resolution to detect these predicted structural transitions, but, *unlike x-ray crystallography, EPR also has the sensitivity and specificity to monitor these same structural states in solution (Ostap et al., 1993) and in the complex lattice of the contracting muscle fiber.* Our results clearly demonstrate that the myosin head in relaxation and contraction has resolved structural states with unique internal molecular dynamics, and the occupancy of these dynamic states is determined by the population of specific biochemical intermediates (Fig. 7). It is not clear that these structural states correlate directly with those predicted from the x-ray data. For example, a more rigorous test of the head-bending model will require studies on probes at distant sites within the head. However, the relative change in the spectral components correlates with the relative change predicted from the crystal structure, i.e., the spectral component (component 3, predominant in (A)M**·D·P) that is most different from rigor (component 1) correlates with the largest predicted change in the myosin head structure (Rayment et al., 1993b; Fisher et al., 1995). Similarly, the two-step increase in rotational disorder that we observe by EPR also correlates with the two-step increase in entropy that occurs when myosin binds and then splits ATP (Kodama, 1988).

Conclusions

In relaxation, the EPR spectrum of IASL-fibers resolves two motionally distinct conformational states within the myosin head, which are predominant in the M·ATP and M·ADP·P_i biochemical intermediates. In contraction, the EPR spectrum reports the same two conformational states observed in relaxation plus a third component that has the same conformational state as rigor. This rigor-like conformational state of the myosin head is a calcium-dependent, actin-bound

state that may represent cross-bridges in the force-generating state. We propose that these internal conformational transitions are coupled to large-scale structural changes within the myosin head, and to changes in the global orientation of actin-attached heads, resulting in the production of force in muscle contraction. Additional steady-state and transient EPR experiments, correlated with transient mechanical and biochemical studies, will be required to test and refine this model.

We thank C. A. Miller and K. Beyzavi for their excellent technical assistance and R. L. H. Bennett, F. L. Nisswandt, and E. Howard for computer assistance.

This work was supported by grants to D.D.T. from the National Institutes of Health (AR32961) and the Minnesota Supercomputer Institute. E.M.O. was supported by a predoctoral training grant from National Institutes of Health (GM08277–03) and National Science Foundation Research Training Grant (DIR-9113444).

REFERENCES

Aguirre, R., S. H. Lin, F. Gonsoulin, C. K. Wang, and H. C. Cheung. 1989. Characterization of the ethenoadenosine diphosphate binding site of myosin subfragment 1 energetics of the equilibrium between two states of the nucleotide · S1 and vanadate-induced global conformation changes detected by energy transfer. *Biochemistry.* 28:799–807.

Bagshaw, C. R., J. F. Eccleston, F. Eckstein, R. S. Goody, H. Gutfreund, and D. R. Trentham. 1974. The magnesium ion-dependent adenosine triphosphate of myosin: two-step processes of adenosine triphosphate association and adenosine diphosphate dissociation. *Biochem. J.* 141: 351–361.

Barnett, V. A., and D. D. Thomas. 1987. Resolution of conformational states of spin-labeled myosin during steady-state ATP hydrolysis. *Biochemistry.* 26:314–323.

Barnett, V. A., and D. D. Thomas. 1989. Microsecond rotational motion of spin-labeled myosin heads during isometric contraction. *Biophys. J.* 56:517–523.

Bell, M. G., J. J. Matta, D. D. Thomas, and Y. E. Goldman. 1993. Changes in cross-bridge kinetics induced by SH-1 modification in rabbit psoas fibers. *Biophys. J.* 64:A252.

Berger, C. L., and D. D. Thomas. 1991. Rotational dynamics of actin-bound intermediates in the myosin ATPase cycle. *Biochemistry.* 30: 11036–11045.

Berger, C. L., and D. D. Thomas. 1993. Rotational dynamics of actin-bound myosin heads in active myofibrils. *Biochemistry.* 32:3812–3821.

Berger, C. L., and D. D. Thomas. 1994. Rotational dynamics of actin-bound intermediates of the myosin ATPase cycle in myofibrils. *Biophys. J.* 67:250–261.

Berger, C. L., E. C. Svensson, and D. D. Thomas. 1989. Photolysis of caged ATP induces microsecond rotation of myosin heads on actin. *Proc. Natl. Acad. Sci. USA.* 86:8753–8757.

Brenner, B., L. C. Yu, and J. M. Chalovich. 1991. Parallel inhibition of active force and relaxed fiber stiffness in skeletal muscle by caldesmon: implications for the pathway to force generation. *Proc. Natl. Acad. Sci. USA.* 88:5739–5734.

Cooke, R. 1986. *Crit. Rev. Biochem.* 21:53–118.

Cooke, R., M. S. Crowder, and D. D. Thomas. 1982. Orientation of spin labels attached to cross-bridges in contracting muscle fibers. *Nature.* 300:776–778.

Crowder, M. S., and R. Cooke. 1984. The effect of myosin sulphydryl modification on the mechanics of fibre contraction. *J. Muscle Res. Cell Motil.* 5:131–146.

Dalbey, R. E., J. Weiel, and R. G. Yount. 1983. Forster energy transfer measurements of thiol-1 to thiol-2 distances in myosin subfragment 1. *Biochemistry.* 22:4696–4706.

Dantzig, J. A., and Y. E. Goldman. 1985. Suppression of muscle contraction by vanadate. *J. Gen. Physiol.* 86:305–327.

Dantzig, J. A., Y. E. Goldman, N. C. Millar, and E. Homsher. 1992. Reversal of the cross-bridge force-generating transition by photogeneration of phosphate in rabbit psoas muscle fibres. *J. Gen. Physiol.* 451: 247–278.

Dantzig, J. A., J. W. Walker, D. R. Trentham, and Y. E. Goldman. 1988. Relaxation of muscle fibers with adenosine 5′-[γ-thio]triphosphate (ATP[γ S]) and by laser photolysis of caged ATP[γ S]: evidence for Ca^{2+}-dependent affinity of rapidly detaching zero-force cross-bridges. *Proc. Natl. Acad. Sci. USA.* 85:6716–6720.

Duke, J., R. Takashi, K. Ue, and M. Morales. 1976. Reciprocal activities of specific thiols when actin binds to myosin. *Proc. Natl. Acad. Sci. USA.* 73:302–306.

Eisenberg, E., and T. L. Hill. 1985. Muscular contraction and free energy transduction in biological systems. *Science.* 227:999–1006.

Fajer, P. G., E. A. Fajer, N. J. Brunsvold, and D. D. Thomas. 1988. Effects of AMPPNP on the orientation and rotational dynamics of spin-labeled muscle cross-bridges. *Biophys. J.* 53:513–524.

Fajer, P. G., R. L. H. Bennett, C. F. Polnaszek, E. A. Fajer, and D. D. Thomas. 1990a. General method for multiparameter fitting of high-resolution EPR spectra using a simplex algorithm. *J. Magn. Reson.* 88:111–125.

Fajer, P. G., E. A. Fajer, J. J. Matta, and D. D. Thomas. 1990b. Effect of ADP on the orientation of spin-labeled myosin heads in muscle fibers: a high resolution study with deuterated spin labels. *Biochemistry.* 29: 5865–5871.

Fajer, P. G., E. A. Fajer, and D. D. Thomas. 1990c. Myosin heads have a broad orientational distribution during isometric muscle contraction. Time-resolved EPR studies using caged ATP. *Proc. Natl. Acad. Sci. USA.* 87:5538–5542.

Fajer, P. G., E. A. Fajer, M. Schoenberg, and D. D. Thomas. 1991. Orientational disorder and motion of weakly attached cross-bridges. *Biophys. J.* 60:642–649.

Ferenczi, M. A. 1986. Phosphate burst in permeable muscle fibers of the rabbit. *Biophys. J.* 50:471–477.

Ferenczi, M. A., E. Homsher, and D. R. Trentham. 1984. The kinetics of magnesium adenosine triphosphate cleavage in skinned muscle fibres of the rabbit. *J. Physiol.* 352:575–599.

Fisher, A. J., C. A. Smith, J. K. Thoden, R. Smith, K. Sutoh, H. M. Holden, and I. Rayment. 1995. Structural studies of myosin:nucleotide complexes: a revised model for the molecular basis of muscle contraction. *Biophys. J.* 68:19s-28s.

Goodno, C. C. 1979. Inhibition of myosin ATPase by vanadate ion. *Proc. Natl. Acad. Sci. USA.* 76:2620–2624.

Goody, R. S., and W. Hofmann. 1980. Stereochemical aspects of the interaction of myosin and actomyosin with nucleotides. *J. Muscle Res. Cell Motil.* 1:101–115.

Hibberd, M. G., and D. R. Trentham. 1986. Relationships between chemical and mechanical events during muscular contraction. *Annu. Rev. Biophys. Biophys. Chem.* 15:119–161.

Highsmith, S., and D. Eden. 1990. Ligand-induced myosin subfragment 1 global conformational change. *Biochemistry.* 29:4087–4093.

Highsmith, S., and D. Eden. 1993. Myosin-ATP chemomechanics. *Biochemistry.* 32:2455–2458.

Hirose, K., T. D. Lenart, J. M. Murray, C. Franzini-Armstrong, and Y. E. Goldman. 1993. Flash and smash: rapid freezing of muscle fibers activated by photolysis of caged ATP. *Biophys. J.* 65:397–408.

Huston, E. E., J. C. Grammer, and R. G. Yount. 1988. Flexibility of the myosin heavy chain: direct evidence that the region containing SH_1 and SH_2 can move 10 Å under influence of nucleotide binding. *Biochemistry.* 27:8945–8952.

Huxley, A. F., and R. Simmons. 1971. Proposed mechanism of force generation in striated muscle. *Nature.* 233:533–538.

Huxley, H. E. 1969. The mechanism of muscular contraction. *Science.* 114:1356–1366.

Huxley, H. E., and M. Kress. 1985. Crossbridge behavior during muscle contraction. *J. Muscle Res. Cell Motil.* 6:153–161.

Katayama, E. 1989. The effects of various nucleotides on the structure of actin-attached myosin S-1 studied by quick-freeze deep-etch electron microscopy. *J. Biochem.* 106:751–770.

Kodama, T. 1988. Stopped-flow calorimetry of myosin ATP hydrolysis: an implication of chemomechanical energy transduction. *Adv. Exp. Med. Biol.* 226:671–676.

Kraft, T., L. C. Yu, H. J. Kuhn, and B. Brenner. 1992. Effect of Ca^{2+} on weak cross-bridge interaction with actin in the presence of adenosine 5′-[γ-thio]triphosphate. *Proc. Natl. Acad. Sci. USA.* 89:11362–11366.

Kress, M., H. E. Huxley, A. R. Faruqi, and J. Hendrix. 1986. Structural changes during activation of frog muscle studied by time-resolved x-ray diffraction. *J. Mol. Biol.* 188:325–342.

Lanzetta, P. A., L. J. Alvares, P. S. Reinach, and O. A. Candia. 1979. *Anal. Biochem.* 100:95–97.

Matta, J. J. 1994. Biochemical and mechanical effects of spin-labeling muscle fibers. Ph.D. thesis. University of Minnesota, Minneapolis, MN. 138 pp.

Matta, J. J., and D. D. Thomas. 1992. Biochemical and mechanical effects of spin-labeling myosin S1. *Biophys. J.* 61:A295.

McCalley, R. C., E. J. Shimshick, and H. M. McConnell. 1972. The effect of slow rotational motion on paramagnetic resonance spectra. *Chem. Phys. Lett.* 13:115–119.

Morita, F. 1967. Interaction of heavy meromyosin with substrate. *J. Biol. Chem.* 242:4501–4506.

Ostap, E. M., H. D. White, and D. D. Thomas. 1993. Transient detection of spin-labeled myosin subfragment 1 conformational states during ATP hydrolysis. *Biochemistry.* 32:6712–6720.

Pollard, T. D., D. Bhandari, P. Maupin, D. Wachsstock, A. G. Weeds, and H. G. Zot. 1993. Direct visualization by electron microscopy of the weakly bound intermediates in the actomyosin ATPase cycle. *Biophys. J.* 64:454–471.

Poole, K. J. V., Y. Maeda, G. Rapp, and R. S. Goody. 1991. Dynamic x-ray diffraction measurements following photolytic relaxation and activation of skinned rabbit psoas fibres. *Adv. Biophys.* 27:63–75.

Rayment, I., H. M. Holden, M. Whittaker, C. B. Yohn, M. Lorenz, K. C. Holmes, and R. A. Milligan. 1993b. Structure of the actin-myosin complex and its implications for muscle contraction. *Science.* 261: 58–65.

Rayment, I., W. R. Rypniewski, K. Schmidt-Bäse, R. Smith, D. R. Tomchick, M. M. Benning, D. A. Winklemann, G. Wesenberg, and H. M. Holden. 1993a. Three-dimensional structure of myosin subfragment-1: a molecular motor. *Science.* 261:50–58.

Reedy, M. K., K. C. Holmes, and R. T. Tregear. 1965. Induced changes in orientation of the cross-bridge glycerinated insect flight muscle. *Nature.* 297:1276–1280.

Reisler, E., M. Burke, and W. F. Harrington. 1974. Cooperative role of two sulfhydryl groups in myosin adenosine triphosphatase. *Biochemistry.* 13:2014–2022.

Roopnarine, O., K. Hideg, and D. D. Thomas. 1993. Saturation transfer EPR spectroscopy with an indane dione spin label: calibration with hemoglobin and application to myosin rotational dynamics. *Biophys. J.* 64:1896–1907.

Roopnarine, O., and D. D. Thomas. 1994. A spin label that binds to myosin heads in muscle fibers with its principal axis parallel to the fiber axis. *Biophys. J.* 67:1634–1645.

Roopnarine, O., and D. D. Thomas. 1995. Orientational dynamics of indane dione spin-labeled myosin head in relaxed and contracting skeletal muscle fibers. *Biophys. J.* 68:1461–1471.

Seidel, J. C., M. Chopek, and J. Gergely. 1970. Effect of nucleotides and pyrophosphate on spin labels bound to S1 thiol groups of myosin. *Biochemistry.* 9:3265–3272.

Sekine, T., and W. W. Kielly. 1964. The enzymatic properties of *N*-ethylmaleimide modified myosin. *J. Biochem. (Tokyo).* 54:196–198.

Shriver, J. W., and B. D. Sykes. 1982. Energetics of the equilibrium between two nucleotide-free myosin subfragment 1 states using fluorine-19 nuclear magnetic resonance. *Biochemistry.* 21:3022–3028.

Sleep, J. A., K. M. Trybus, K. A. Johnson, and E. W. Taylor. 1981. Kinetic studies of normal and modified heavy meromyosin and subfragment-1. *J. Muscle Res. Cell Motil.* 2:373–399.

Squier, T. C., and D. D. Thomas. 1989. Selective detection of the rotational dynamics of the protein-associated lipid hydrocarbon chains in sarcoplasmic reticulum membranes. *Biophys. J.* 56:735–748.

Stein, R. A., R. D. Ludescher, P. S. Dahlberg, R. L. Bennett, P. G. Fajer, and D. D. Thomas. 1990. Time-resolved rotational dynamics of phosphorescent-labeled myosin heads in contracting muscle fibers. *Biochemistry.* 29:10023–10031.

Sutoh, K., and R. C. Lu. 1987. Identification of two segments, separated by ~45 kilodaltons, of the myosin subfragments 1 heavy chain that can be cross-linked to the SH-1 thiol. *Biochemistry.* 26:4511–4516.

Taylor, E. W. 1979. Mechanism of actomyosin ATPase and the problem of muscle contraction. *CRC Crit. Rev. Biochem.* 6:103.

Thomas, D. D. 1994. Angular disorder of weak-binding actomyosin cross-bridges. *Biophys. J.* 66:1272–1273.

Thomas, D. D., and R. Cooke. 1980. Orientation of spin-labeled myosin heads in glycerinated muscle fibers. *Biophys. J.* 32:891–906.

Thomas, D. D., S. Ishiwata, I. Seidel, and J. Gergely. 1980. Submillisecond rotational dynamics of spin-labeled myosin heads in myofibrils. *Biophys. J.* 32:873–890.

Thomas, D. D., S. Ramachandran, O. Roopnarine, D. W. Hayden, and E. M. Ostap. 1995. The mechanism of force generation in myosin: a disorder-to-order transition, coupled to internal structural changes. *Biophys. J.* 68:135s–141s.

Thomas, D. D., J. C. Seidel, J. S. Hyde, and J. Gergely. 1975. Motion of subfragment-1 in myosin and its supramolecular complexes: saturation transfer electron paramagnetic resonance. *Proc. Natl. Acad. Sci. USA.* 72:1729–1733.

Tokunaga, M., K. Sutoh, and T. Wakabayashi. 1991. Structure and structural change of the myosin head. *Adv. Biophys.* 27:157–167.

Trentham, D. R., J. F. Eccleston, and C. R. Bagshaw. 1976. Kinetic analysis of ATPase mechanisms. *Q. Rev. Biophys.* 9:217–281.

Wakabayashi, K., M. Tokunaga, I. Kohno, Y. Sugimoto, T. Hamanaka, Y. Takezawa, T. Wakabayashi, and Y. Amemiya. 1992. Small-angle synchrotron x-ray scattering reveals distinct shape changes of the myosin head during hydrolysis of ATP. *Science.* 258:443–447.

Walker, M., and J. Trinick. 1988. Visualization of domains in native and nucleotide-trapped myosin heads by negative staining. *J. Muscle Res. Cell Motil.* 9:359–366.

Walker, M., H. White, B. Belknap, and J. Trinick. 1994. Electron cryomicroscopy of acto-myosin-S1 during steady state ATP hydrolysis. *Biophys. J.* 66:1563–1572.

Walker, M., J. Trinick, and H. White. 1995. Millisecond time-resolution electron cryomicroscopy of the M-ATP transient kinetic state of the actomyosin ATPase. *Biophys. J.* 68:87s–91s.

Wells, C., and C. R. Bagshaw. 1984. The characterization of vanadate-trapped nucleotide complexes with spin-labelled myosins. *J. Muscle Res. Cell Motil.* 5:97–112.

Werber, M., A. G. Szent-Györgyi, and G. Fasman. 1972. Fluorescence studies on heavy meromyosin-substrate interaction. *Biochemistry.* 11: 2872–2882.